Hardware-in-the-Loop Protection Validation for Dominion Energy Blackstart Operations

Sergio A. Dorado-Rojas*†, Luigi Vanfretti*
*Rensselaer Polytechnic Institute
Troy, NY, USA
{dorads, vanfrl}@rpi.edu
†University of Connecticut
Storrs, CT, USA
sergio.dorado@uconn.edu

Xiawen Li, Micah J. Till, Kevin D. Jones, Matthew Gardner
Dominion Energy
Electric Transmission Operations
Richmond, VA, USA
{xiawen.li, micah.j.till, kevin.d.jones
matthew.gardner}@dominionenergy.com

***Abstract*—This article assesses transformer differential protection and out-of-step blocking (OOSB) schemes during blackstart in Dominion Energy's system. The protective functions are validated by hardware-in-the-loop (HIL) simulations involving the relay hardware with the configurations deployed on the field. A dditionally, w e i ntroduce a systematic methodology to generate OOSB testing scenarios based on the analytic linearization of the system dynamical model. Our results show that both protective functions perform satisfactorily despite the weak grid condition of the network during restoration.**

***Index Terms*—blackstart, differential protection, hardware-in-the-loop, HIL, out-of-step blocking, OOSB, real-time simulation**

I. Introduction

Modern power grids have elaborate protection systems that provide safe and secure electric transmission worldwide. Yet low-probability events can have an outsized effect on the grid's stability, including catastrophic weather, cyber-attacks, and physical attacks. Restoration from a blackout, called a *blackstart*, is a process that must achieve a two-fold objective [1], [2]: it shall maximize the share of restored service while minimizing the elapsed time. A blackstart procedure is subject to several constraints, such as system dynamics, power flow limits throughout the system, and load priority.

Restoration is typically considered during the design and operation of a power system. An electric energy system is conceived to operate in one of the five f undamental s tates, as shown in Fig. 1 [3]. While power system operators aim to maintain the normal system state, a reliable grid must have a clear operating plan for all possible conditions. Restoration is a critical action that the generation and transmission owners must provide [4], [5].

In compliance with NERC *EOP-005-3* and PJM *Manual 36*, Dominion's System Restoration Plan (SRP) specifies the company's blackstart procedures, identifying the blackstart units (BSUs) and the different cranking paths.

Dominion's SRP follows the core-island technique (Fig. 2). This technique requires the formation of a core island which is a stable but electrically weak system. The underlying method attempts to form a relatively highly meshed, stable

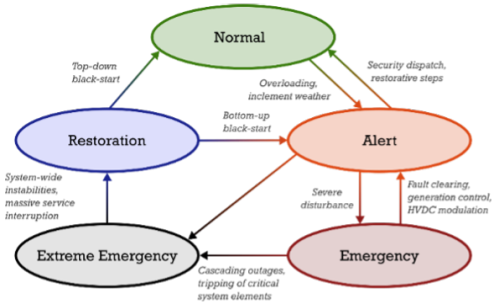

Fig. 1: Operating conditions in a grid (adapted from [3]).

island while supplying critical loads as soon as possible. The resulting stable island can also be connected to neighboring utilities more quickly, which leads to a more significant fault current capacity and small clearing times, thus strengthening the security margins of the system.

Among the numerous studies associated with the SRP, one of the most critical analyses examines the performance of protective equipment during restoration [6]–[10]. In the early stages of a blackstart maneuver, the electrical island is electrically weaker than the system is during regular operation. Because relay characteristics are set up by contingency analysis on the grid under normal conditions, it is not guaranteed that protective equipment will operate adequately during restoration.

Several investigations concerning the steady-state and dynamic behavior of the system support blackstart procedures (e.g., [11]), with real-time (RT) simulation gaining more relevance as a decision-making support tool [12], [13]. Likewise, RT simulation has also been used to validate protective relaying performance [14]. Despite its capabilities, RT simulation alone would require substantial efforts to re-implement the relay logic of interest. While commercial simulators offer a plethora of built-in protective functions as software models of different relay functions. However, the behavior of such models can differ from the functionality deployed on an actual relay so that the accuracy of the results

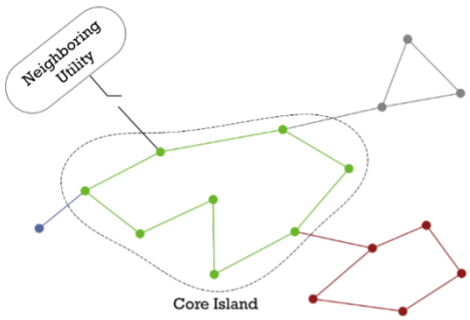

Fig. 2: Core-island bottom-up blackstart restoration.

is compromised [14]. Software RT simulation protective models do not generally include practical characteristics of physical relays, such as the Analog-to-Digital Conversion (ADC) processes and internal communications that may compromise their performance (e.g., [15]). Neglecting those aspects compromises the fidelity of the software RT model. For instance, in [16], the authors show different tripping times between a physical relay and its RT software model.

Hardware-in-the-Loop (HIL) simulation emerges as an alternative to perform more accurate studies to validate relay performance. HIL allows interaction with the actual relay hardware so that the protection logic in the validation study is the same as deployed on the field. HIL validation of blackstart procedures (e.g., [17]) and HIL-based protection assessment (e.g., [10], [16], [18]) are receiving increasing attention within the power system community.

While acknowledging the relevance of protection studies during blackstart, the primary purpose of this work is to assess via HIL simulation the performance of protective schemes for transformers and transmission lines on the 500 kV level during energization. The cranking path of interest starts from a 230 kV BSU to a 500 kV nuclear unit, with different load pick-up paths at the 230 kV level (Fig. 3).

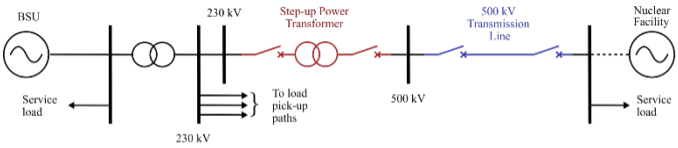

Fig. 3: Cranking path of interest from the Dominion SRP.

We were concerned about two relay protective functions: transformer differential protection and transmission line out-of-step distance protection (more specifically, out-of-step blocking). We performed our experiments on an RT simulation model in RSCAD using the cranking path dynamical model. The RTDS hardware interfaced via a power amplifier to the actual relay, which sent the breaker control signals back to the input/output ports of the RT simulator. The relays used in this study were an SEL-421 (for transmission line distance protection) and an SEL-487E (for transformer differential protection). The experiment layout is shown in Fig. 4.

This paper is structured as follows. Section II introduces the protection functions assessed in this work: transformer

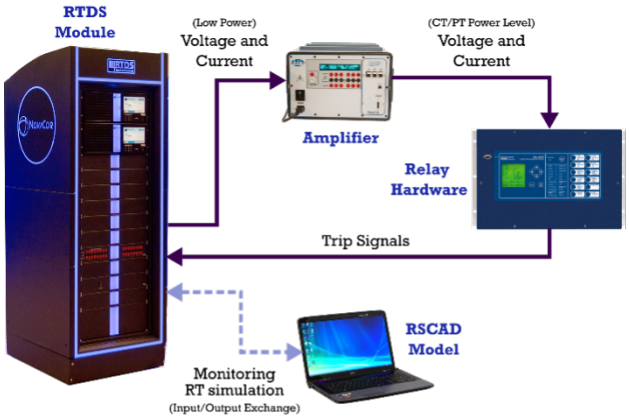

Fig. 4: HIL experiment layout for protection function validation.

differential protection and out-of-step blocking. Experiment design to generate out-of-step cases is described in Section III. Results are presented in Section IV. Finally, the work is concluded in Section V.

II. Protection Concepts

A. Transformer Differential Protection

Current-based differential protection compares the currents flowing in and out of a protection zone (I_p and I_s in Fig. 5). If the difference between the Current Transformer (CT) readings, or differential current $I_1 - I_2$, exceeds a given threshold, corrective action is taken. The current flow through the protected device is interrupted by opening the corresponding circuit breakers. Such a disbalance arises because of an event within the protection zone, what is known as an internal fault.

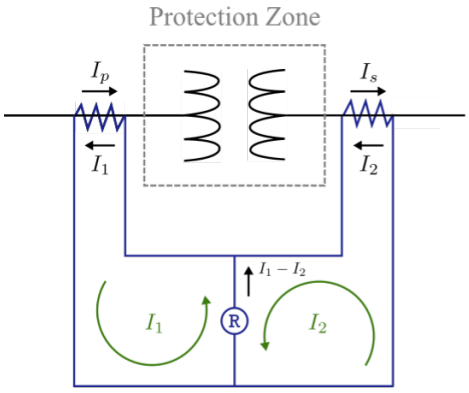

Fig. 5: Current-based differential protection for a transformer.

Assuming perfect CTs, an ideal differential protection scheme is the most selective because it responds only to faults within its protection zone. In practice, a differential current may exist under normal conditions due to a mismatch between the CT ratios of the primary and secondary sides and magnetic core saturation during heavily loaded conditions and external faults [19], [20]. Since these currents flow through the measurement circuit but do not correspond to

an actual differential current on the transformer windings, they are known as false differential currents. The percentage restrained differential protection scheme overcomes most of the practical challenges of the ideal differential scheme [21]. A percentage restraint differential relay operates as a function of two quantities: the operate current I_{OP} and the through or restraint current I_{R}. The operate current corresponds to the differential current in the protection zone and is computed as:

$$I_{\mathrm{OP}} \coloneqq I_1 - I_2. \tag{1}$$

The restraint current is a function of the winding currents. Several definitions are possible for I_R, with the most common ones being average restraint and maximum restraint [10]. The average restraint corresponds to a weighted average of the current magnitudes,

$$I_{R,\mathrm{avg}} = k\left(|I_1| + |I_2|\right) \tag{2}$$

where k is a slope or weighting factor. Likewise, the maximum restraint corresponds to the maximum magnitude of I_1 and I_2:

$$I_{R,\max} = \max\left(|I_1|, |I_2|\right). \tag{3}$$

The relay action is based on whether I_{OP} exceeds I_R or not. Therefore, to a great extent, the definition of the restraint current characterizes the relay differential functionality. With either definition of I_R, the simplest tripping rule of a percentage restraint relay is

$$I_{\mathrm{OP}} \geq \kappa I_R \tag{4}$$

where κ is the slope of the percentage characteristic. As shown in Fig. 6, a bias or minimum pickup is set to compensate for a false differential current. The higher the bias, the less sensitive the relay is to CT saturation and measurement errors.

As in Fig. 6, an adaptive slope strategy changes its selectivity threshold based on the level of I_R. In other words, the relay characteristic becomes steeper when the current flowing through the transformer exceeds a given magnitude. The larger the current flowing through the transformer, the more sensitive the relay is to external faults [19], [20].

Therefore, when I_R becomes too large, the relay will command the associated circuit breakers to protect the transformer. An adaptive slope setting enhances the system security since it widens the boundary of the protection zone for a large I_R. The relay will react to external events that cause the fault currents to flow through the transformer windings. Such a characteristic has remarkable importance during blackstart conditions since there is no guarantee that all relaying devices providing overarching protection zones will be online and operating when the maneuver is executed.

During transformer energization, the in-rush current required to magnetize the transformer core exceeds by several orders of magnitude the nominal current of the device. Moreover, since such current flows only through the primary, it can result in a non-zero differential reading. The in-rush current is known to have a rich harmonic component [19], [20]. So, harmonic restraint schemes are used within differential protections to discard tripping during energization by analyzing the harmonics of the in-rush current.

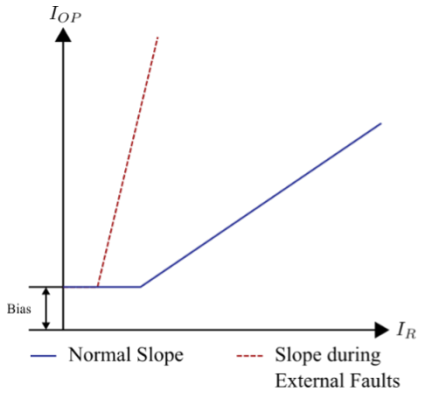

Fig. 6: Adaptive slope characteristic for differential protection.

B. Distance and Out-of-Step Protection

Distance relays. Since assets such as transmission lines span a significant geographic area, a differential scheme is no longer feasible for protection. In such cases, distance relays can be effective. A distance relay takes advantage of the fact that a transmission line's impedance per unit length is relatively constant. By monitoring the impedance seen by the relay, or $\tilde{Z}_R = \tilde{V}_R/\tilde{I}_R$, after a fault occurs, the protection logic determines whether a tripping action is required or not.

Since $\tilde{Z}_R$ is used as a decision variable in distance protection schemes, protection zones are specified as loci on the complex resistance-reactance $R - X$ plane. Inspired by electromechanical relays, loci such as mho circles and blinders are still used to specify distance relay curves (see Fig. 7) [22].

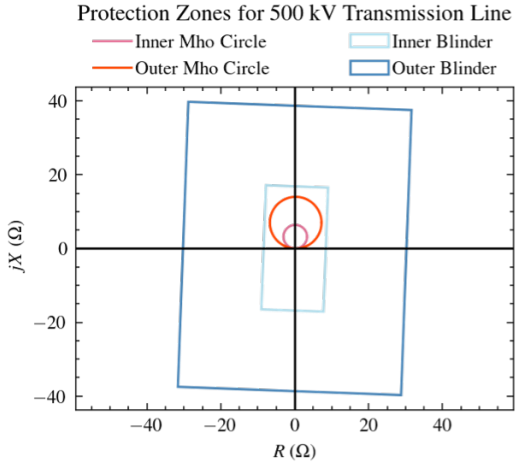

Fig. 7: Protection zones for a 500 kV transmission line.

Under normal conditions, the impedance seen by the relay is outside the $R - X$ loci. Then, when a large disturbance such as a fault happens, $\tilde{Z}_R$ changes rapidly and, if it falls inside the protection loci, a tripping action is issued. However, oscillations arising after a small disturbance can produce

slower impedance changes. The rate of change of $\tilde{Z}_R$ is determined by the underlying dynamics of the system.

Out-of-step blocking. OOSB is used in a scenario where a stable power oscillation occurs through the line. In this case, the impedance seen by the relay may enter the protected region but then leaves it as the oscillation fades out. So, the relays should not open the breakers at each end of the transmission line since the oscillation will eventually dampen out, and the system will return to a safe steady-state.

III. Experiment Scenario Generation

Our experiment design for OOSB went beyond short-circuit experiments. Out-of-step validation requires small disturbances to generate power swings. Below, we outline a linear analysis-based technique that analytically generates such scenarios.

Consider a network whose electromechanical dynamics are represented by a swing equation, and the Automatic Voltage Regulator (AVR) and exciter dynamics are included explicitly:

$$\begin{aligned} \frac{2H}{\omega_s}\frac{d^2}{dt^2}[\delta(t)] &= P_m(t) - P_e(t) - \frac{D}{\omega_s}\frac{d}{dt}[\delta(t)], \\ P_e(t) &= \frac{V_1(t)V_2(t)}{X_{12}}\sin\delta(t), \\ \dot{V}_1 &= f_{\text{AVR}}\left(V_1, V_1^*\right). \end{aligned} \tag{5}$$

In (5), H is the aggregated inertia constant, ω_s is the base frequency, D is the load damping coefficient, $P_m(t)$ is the perunit shaft mechanical power, $P_e(t)$ is the electrical power flow, and V_1, V_2 are the Thévenin voltages at the sending and receiving ends of the transmission line, respectively, and f_{AVR} is a nonlinear function describing the AVR and exciter dynamics. V_1^* is the reference for the V_1 voltage.

Note that the electric power $P_e(t)$ was assumed to flow through a lossless transmission line. We can see that, after a disturbance, the power flow through the line will change depending on the phase angle $\delta(t)$ (i.e., $P_e(t) = P_e(\delta(t))$) so that the impedance rate of change seen by the relay depends on the time constant of (5). Such dynamical behavior produces impedance trajectories in the $R - X$ plane, which could be stable or unstable depending on the Lyapunov stability of (5) about $\delta\left(t = t_0\right) = \delta_0$ at the onset of the perturbation.

The nonlinear system in (5) can be written as $\dot{\mathbf{x}} = \mathbf{f}(\mathbf{x}, \mathbf{u})$; $\mathbf{y} = \mathbf{g}(\mathbf{x}, \mathbf{u})$ with $\mathbf{x}$ being the state vector, $\mathbf{u}$ as the vector of inputs, $\mathbf{y}$ as the measurements, and $\mathbf{f}, \mathbf{g}$ as two nonlinear functions. Let the pre-disturbance state vector be $\mathbf{x}_0$. Under mild assumptions (small variations), the system can be analytically linearized as $\mathbf{A} := \partial\mathbf{f}/\,\partial\mathbf{x}|_{\mathbf{x}=\mathbf{x}_0}$, $\mathbf{B} := \partial\mathbf{f}/\,\partial\mathbf{u}|_{\mathbf{x}=\mathbf{x}_0}$, and $\mathbf{C} := \partial\mathbf{g}/\,\partial\mathbf{x}|_{\mathbf{x}=\mathbf{x}_0}$. Using these matrices, the transfer function of the system is computed as $\mathbf{G}(s) = \mathbf{C}(s\mathbf{I} - \mathbf{A})^{-1}\mathbf{B}$. From this transfer function matrix, we take the component describing the system from input V_1^* to output V_1, written as $G_{\text{AVR}}(s)$. In other words, we are interested in the input-output dynamics as seen from the AVR. We aim to compute the sensitivity of the AVR's integral gain K_{IR}. This is obtained from the root-locus of $G_{\text{AVR}}(s)$ when varying K_{IR}, as shown in Fig. 8 by the green trace.

The AVR gain is varied to reduce the damping of the system. So, a lightly damped stable power swing occurs after a small disturbance is applied to the system (Fig. 9). While such a change in K_{IR} was intentional for experiment design, it can arise in practice due to the mistuning of machine controls following a cyber-attack on a generation unit's SCADA system.

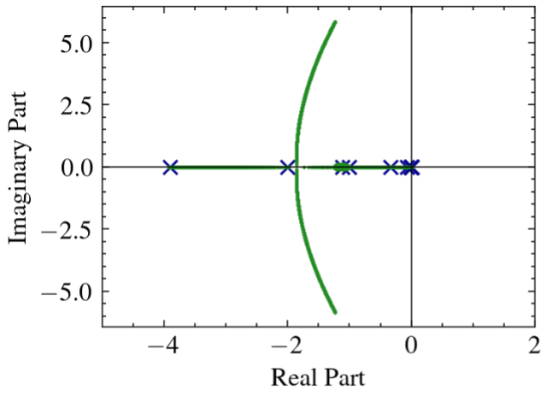

Fig. 8: Root locus for AVR's integral gain variation.

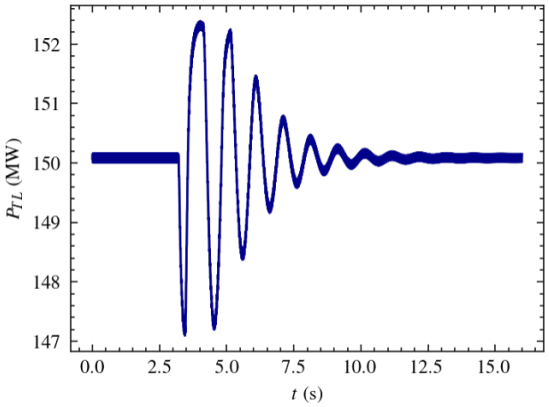

Fig. 9: Power swing generated by varying the AVR gain.

IV. Results

During a blackstart, the magnetizing in-rush current did not result in undesired tripping despite the flow of operate current (Fig. 10a). This confirmed experimentally that the harmonic restraint settings of the differential protection were adequate for the substation of interest. Furthermore, as shown in Fig. 10b, when the fault occurred outside the protection zone but the current flowed through the transformer, a tripping action was issued thanks to the adaptive slope characteristic. This will help prevent further damage to a transformer in the extreme case where overcurrent protections are offline during restoration.

Fig. 11 shows an impedance trajectory for a stable scenario we produced to evaluate OOSB. In this case, for a "heavy" load condition (i.e., several MW flowing through the line during a blackstart), we observe that trajectories are at a considerable distance from the protection region in the plane.

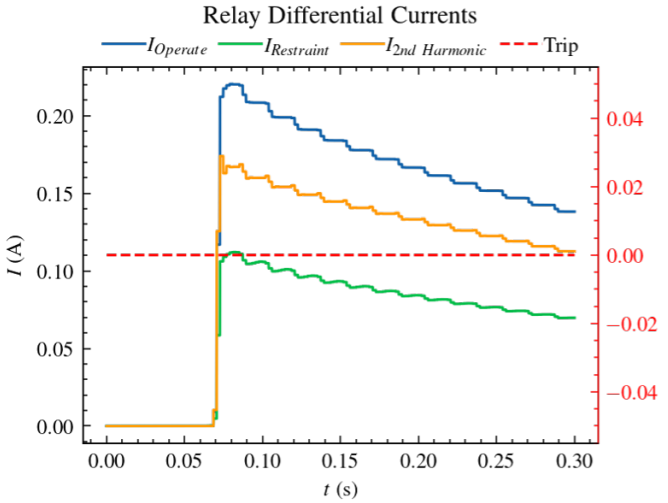

(a) Differential current during transformer energization.

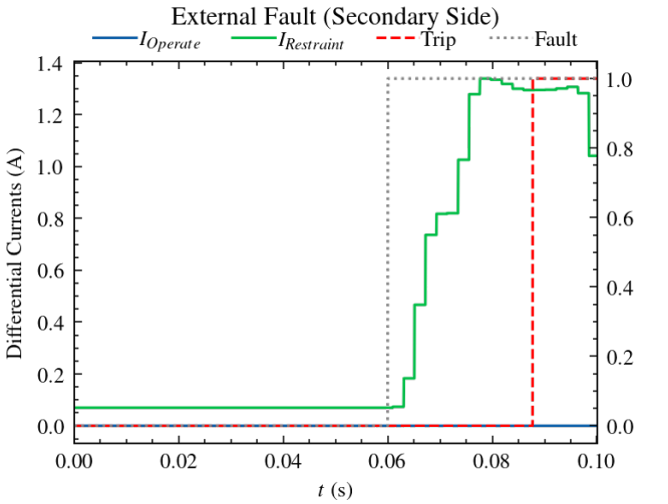

(b) Currents during external faults on the secondary side.

Fig. 10: Differential currents during different experiments.

As the load increases further, the trajectories swing closer to the protection zone. However, according to the SRP, such a load increase during restoration will be accompanied by generation reconnection. So the system's damping will also increase, decreasing the likelihood of a stable power swing "strong" enough for an impedance excursion through the protection zones. Hence, the normal conditions OOSB settings can be used safely during a blackstart in this particular substation.

V. Conclusions

This study validated two protective functions used during a blackstart via HIL simulation on a cranking path at the 500 kV level. Thanks to HIL, we could verify the performance of the exact settings deployed on the field in the same relay hardware while emulating the restoration procedure in an RT simulator.

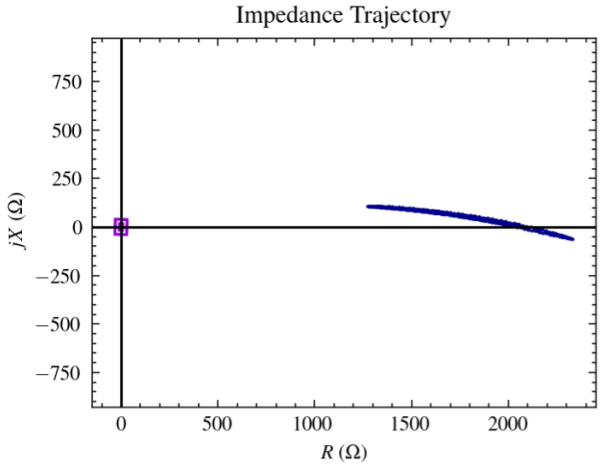

Fig. 11: Impedance trajectory during a stable power swing for out-of-step evaluation.

We confirmed that the protective settings are adequate for the differential protection scheme outlined in Dominion's SRP since the performance was as expected for energization and internal and external faults. For OOSB, we proposed an analytic methodology to generate testing scenarios with stable power swings through the transmission line of interest. We found that the loci for impedance trajectories lie far away from the protection zones, so the likelihood of a crossing with the protective region boundaries is small.

While our results speak only to the system under test, our methodology is extensible to any system. Future work concerns the evaluation of out-of-step tripping for unstable power swing scenarios.

Acknowledgments

The authors would like to thank Dr. Zongjie Wang for supporting the presentation of this work.

References

[1] A. Borghetti, C. A. Nucci, and M. Paolone, "Restoration Processes after Blackouts," in *Handbook of Electrical Power System Dynamics: Modeling, Stability, and Control*, M. Eremia and M. Shahidehpour, Eds. John Wiley & Sons, 2013, pp. 864–899.

[2] J. Feltes and C. Grande-Moran, "Down, but Not Out: A Brief Overview of Restoration Issues," *IEEE Power and Energy Magazine*, vol. 12, no. 1, pp. 34–43, Jan. 2014.

[3] P. Kundur, *Power system stability and control*. New York, NY: McGraw-Hill Professional, 1994.

[4] "Power System Restoration Reference Guide," EPRI, Palo Alto, CA, Tech. Rep. 3002019264, 2020.

[5] "Guide to Grid Protection During System Restoration," EPRI, Palo Alto, CA, Tech. Rep. 3002018205, 2020.

[6] H. Xing-Qi, L. Jun-Yong, Y. Ke, and X. Lian-Fang, "Control Strategies of Black-Start," in *2009 Asia-Pacific Power and Energy Engineering Conference*. infona.pl, 2009.

[7] Y. Wang, H.-M. Chou, R. Sun, W. Ju, C. Mishra, and K. Thomas, "Dynamic study of Dominion's system restoration plan in RTDS," in *2019 IEEE Power Energy Society Innovative Smart Grid Technologies Conference (ISGT)*. ieeexplore.ieee.org, Feb. 2019, pp. 1–5.

[8] R. Ilievska, "Real-time dynamic simulation of a power-system restoration process," Ph.D. dissertation, Univerza v Ljubljani, Fakulteta za elektrotehniko, 2019.

[9] B. Niemann, R. Liu, D. Yang, Y. Wang, and A. Pinceti, "Impact of STATCOMs in Dominion Energy's System Restoration Plan," in *2020 IEEE/PES Transmission and Distribution Conference and Exposition (T D)*. ieeexplore.ieee.org, Oct. 2020, pp. 1–6.

[10] M. Ferrari, E. C. Piesciorovsky, T. Smith, and J. Hambrick, "Cost-effective three-phase current amplifier interface for real-time simulator with relays in-the-loop," in *2019 North American Power Symposium (NAPS)*. IEEE, Oct. 2019.

[11] H. Chou, C. Mishra, Y. Wang, and K. Thomas, "Application of RTDS as Real-Time Decision Support Tool," in *Grid of the Future Symposium*. cigre-usnc.org, 2017.

[12] F. Plumptre, S. Brettschneider, A. Hiebert, M. Thompson, and M. Mynam, "Validation of out-of-step protection with a real time digital simulator," in *Proceedings of the 60th Annual Georgia Tech Protective Relaying Conference*, 2006.

[13] Z. Yang, Y. Wang, L. Xing, B. Yin, and J. Tao, "Relay Protection Simulation and Testing of Online Setting Value Modification Based on RTDS," *IEEE Access*, vol. 8, pp. 4693–4699, 2020.

[14] S. A. Dorado-Rojas, X. Li, R. Liu, and M. J. Till, "Transformer Differential Protection Studies for Dominion Energy's Blackstart Operations," in *2021 Grid of the Future Symposium - CIGRÉ USNC*, Sep. 2021.

[15] S. A. Dorado-Rojas, S. Xu, L. Vanfretti, G. Olvera, M. I. I. Ayachi, and S. Ahmed, "Low-Cost Hardware Platform for Testing ML-Based Edge Power Grid Oscillation Detectors," in *2022 10th Workshop on Modelling and Simulation of Cyber-Physical Energy Systems (MSCPES)*, May 2022, pp. 1–6.

[16] M. S. Almas, R. Leelaruji, and L. Vanfretti, "Over-current relay model implementation for real time simulation Hardware-in-the-Loop (HIL) validation," in *IECON 2012 - 38th Annual Conference on IEEE Industrial Electronics Society*. ieeexplore.ieee.org, Oct. 2012, pp. 4789–4796.

[17] R. Liu, R. Sun, and M. Tania, "Hardware-in-the-loop relay testing in dominion's blackstart plan," 2017.

[18] M. S. Almas and L. Vanfretti, "RT-HIL Implementation of the Hybrid Synchrophasor and GOOSE-Based Passive Islanding Schemes," *IEEE Transactions on Power Delivery*, vol. 31, no. 3, pp. 1299–1309, Jun. 2016.

[19] J. L. Blackburn and T. J. Domin, *Protective relaying: principles and applications*. CRC press, 2006.

[20] S. H. Horowitz and A. G. Phadke, *Power System Relaying*. John Wiley & Sons, Apr. 2008.

[21] M. J. Thompson, "Percentage restrained differential, percentage of what?" in *2011 64th Annual Conference for Protective Relay Engineers*. ieeexplore.ieee.org, Apr. 2011, pp. 278–289.

[22] C. R. Mason, "The art and science of protective relaying," *General Electric*, 1956.